A PRIORI DESIGN OF A CONTINUOUS ANNULAR PHOTOCHEMICAL REACTOR: EXPERIMENTAL VALIDATION FOR SIMPLE REACTIONS

ELIANA R. DE BERNARDEZ† and ALBERTO E. CASSANO‡

Instituto de Desarrollo Tecnológico para la Industria Química, Casilla de Correo 91, Guemes 3450, 3000 Santa Fe (Argentina)

(Received August 3, 1984; in revised form December 10, 1984)

Summary

This paper presents a model for a continuous flow annular photoreactor for a simple photochemical reaction. The radiation field is described using the volumetric emission extense source model. Output conversions are computed by solving the mass balance equation and predictions are compared with bench-scale experiments. The model does not use adjustable parameters.

The photodecomposition of an oxalic acid–uranyl sulfate aqueous solution is employed as a test reaction. At short wavelengths, when local values of conversion exceed the recommended maximum value of 20%, the reaction becomes dependent on the oxalic acid concentration because the nature of the uranyl oxalate chemical complex varies. Consequently, the predicted exit conversions are computed using a variable napierian absorption coefficient, which is a function of the spatial distribution of the oxalic acid concentration. They are compared with experimental conversions for two reactors of different radii and show very good agreement. Some deviations are observed when the local values of the oxalic acid conversions are greater than 80%; in this case the published data on quantum yields may no longer be valid.

1. Introduction

Several emission models have been proposed to predict the radiation field inside a photochemical reactor. Two of these, the volumetric emission extense source (VEES) model [1] for non-fluorescent arc-type lamps, and the superficial emission extense source model [2] for fluorescent lamps, result from a rigorous treatment in which all the dimensions of the lamp

†Research Assistant from Consejo Nacional de Investigaciones Cientificas y Técnicas (CONICET).

‡Member of CONICET's Scientific and Technological Research Staff and Professor at Universidad Nacional del Litoral.

0047-2670/85/$3.30

are taken into account. A third type of model considers the tubular lamp to be linear (spherical emission linear source (SELS) model [3]); this should be valid for any type of lamp. Both isotropic or diffuse emission of radiation can be incorporated into the formulation of the three approaches.

Cerdá *et al.* [4] and De Bernardez and Cassano [5] performed several evaluations of the VEES model. Alfano *et al.* [6] conducted a precise verification of its applicability to a system where both direct and indirect radiation were present. It seems appropriate to perform a careful analysis of the precision with which a radiation field can be predicted in a continuous photoreactor where large radiation density flux gradients exist. At the same time, as will be shown below, the results could be used to investigate the possibility of using a uranyl oxalate actinometer for continuous photoreactors in which extreme radiation gradients are present. Experiments could be performed using this approach to check simultaneously the quality of the VEES model and the ability of a chemical actinometer to evaluate absolutely the radiation field inside a practical photoreactor.

2. The reaction system

The optical and kinetic characteristics of the uranyl oxalate actinometer were carefully studied [7 - 10]. It was found that if the molar ratio of oxalic acid to uranyl ions is 2 or greater and the uranyl ion concentration is 0.001 M or greater almost all the radiation is absorbed by uranyl oxalate complexes which decompose into water, carbon dioxide, carbon monoxide and formic acid, while the uranyl ion remains unchanged [10].

Although the quantum yield determinations were made with solutions of 0.01 M uranyl sulfate and 0.05 M oxalic acid, as long as a 5:1 molar ratio is maintained a tenfold decrease in concentration has no effect on the quantum yield [8], while the napierian absorption coefficient decreases in proportion to the dilution. In this work a dilute solution (0.001 M uranyl sulfate and 0.005 M oxalic acid) was used so that the reactor could be operated within an experimentally feasible range of volumetric flow rates.

The rate of the photochemical reaction can be expressed in terms of the volumetric rate of energy absorption and the overall quantum yield which represents the molecules of oxalic acid decomposed per quantum of radiation absorbed by the system [7].

The main overall photochemical reactions are

$$UO_2^{2+} + H_2C_2O_4 + h\nu \longrightarrow UO_2^{2+} + CO_2 + CO + H_2O \quad (1)$$

$$UO_2^{2+} + H_2C_2O_4 + h\nu \longrightarrow UO_2^{2+} + CO_2 + HCOOH \quad (2)$$

Heidt *et al.* [10] pointed out that at low pH (close to 0) the molar ratio of CO produced to oxalic acid decomposed is approximately 1, clearly establishing that under these conditions only reaction (1) is significant. This ratio decreases when the pH is in the range 1 - 3 showing that reaction

(2) is becoming increasingly important. For pH values higher than 6 there is evidence that reaction (1) no longer occurs.

When the quantum yield is expressed with respect to the decomposed oxalic acid, for conversions below 80%, it is independent of the reaction path and has a constant value when the pH is in the range 1 - 5. It has also been established that the reaction is of zeroth order with respect to the oxalic acid concentration if the molar ratio of oxalic acid to uranyl ions is about 5 and if the oxalic acid conversion is kept below 20% [11, 12]. On the other hand, in order to be able to carry out the analysis of the reaction products with the required accuracy, the conversion must be higher than 5%. In addition to these restrictions, the maximum permissible conversion value is limited by the formation of bubbles (CO_2 and CO are reaction products). At shorter wavelengths where the radiation absorption is very high (for instance between 2000 Å and 3000 Å) the bubbles do not lead to significant problems in the evaluation of the napierian absorption coefficient; the effective absorption coefficient when bubbles are present is almost the same as that for pure liquid [13, 14]. This will not be the case at longer wavelengths where the absorption coefficient of the solution rapidly decreases (between 3000 Å and 4000 Å for example). In this case, it was shown that the "effective" absorption coefficient is different [13, 14]. Thus, the distortion of the radiation field produced by the heterogeneities in the reaction volume cannot be neglected.

3. Experimental details

The reaction was carried out in a continuous annular reactor. The radiation was provided by a General Electric G15T8 low pressure germicidal lamp, designed to emit almost all its radiant energy at 2537 Å. Table 1 summarizes the main characteristics of the lamp that are provided by the manufacturer [15].

All parts of the equipment in contact with reactants were made of Pyrex glass, quartz or Teflon. With the exception of the reactor irradiation zone, the system was totally isolated from light.

TABLE 1

Lamp data

Nominal input power (W)	15
Nominal length (cm)	45.7
Effective length of UV source (cm)	35.6
Nominal diameter (cm)	2.54
Approximate lamp current (A)	0.310
Approximate lifetime (h)	7500
Output power at 2537 Å (W)	
at 100 hours	3.6
through life	2.8

Two reactors were used: number 1 ($z_{R2} - z_{R1} = 30$ cm; $r_{in} = 2.3$ cm; $r_{ou} = 2.7$ cm) and number 2 ($z_{R2} - z_{R1} = 30$ cm; $r_{in} = 2.3$ cm; $r_{ou} = 3.6$ cm). r_{in} and r_{ou} are nominal inner and outer radii respectively. The reactor irradiation zone was limited by two masks (Fig. 1) which reduced the nominal reaction length to 30 cm. Owing to the short wavelength of the lamp emission, the reactor inner wall was made of quartz (Suprasil quality). There are no limitations in the material required for the outer wall and hence it was made of Pyrex glass.

The initial concentration of the actinometric solution was 0.005 M oxalic acid (RPE-ACS Carlo Erba) and 0.001 M uranyl sulfate. The latter was prepared by precipitation and successive recrystallization from nuclear grade ammonium uranyl tricarbonate and its purity was checked spectrophotometrically.

The experimental procedure had the following features: (a) continuous monitoring of the lamp operation (voltage, intensity and input power); (b) continuous monitoring of the operating flow rate; (c) permanent control of the concentration of the product stream.

For both inlet and outlet samples, the oxalic acid concentration was measured by permanganimetric titration and the uranyl complex concentration was determined spectrophotometrically. Several samples were taken after the system had achieved steady state conditions with respect to lamp operation, flow rate and temperature. All spectrophotometric measurements were performed using a Cary 17 D spectrophotometer with a 1 cm thick cell using distilled water as a blank.

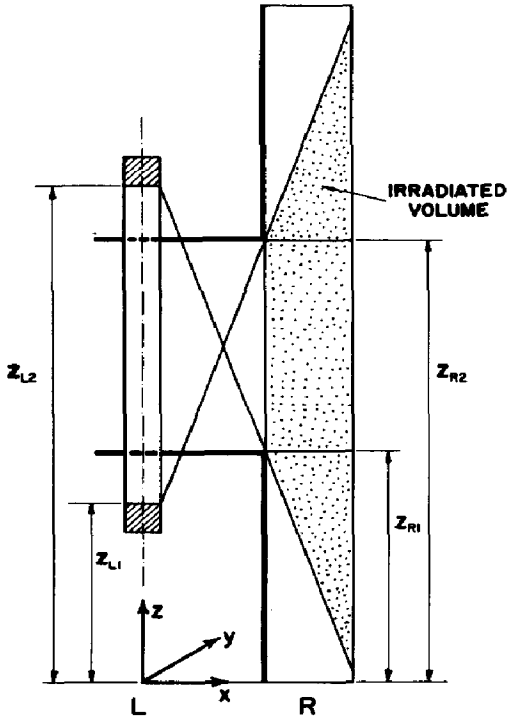

Fig. 1. Reactor geometry.

4. Modelling of the system

The system was studied by assuming the following conditions: (i) a steady state, (ii) negligible thermal effects, (iii) axial laminar flow, (iv) incompressible newtonian fluid behavior, (v) azimuthal symmetry, (vi) negligible axial diffusion when compared with the axial convective flux and (vii) a constant diffusion coefficient.

Hence the mass balance equation for the oxalic acid is

$$v_z(r)\,\frac{\partial C_{ox}}{\partial z} = D_{ox}\,\frac{1}{r}\,\frac{\partial}{\partial r}\left(r\,\frac{\partial C_{ox}}{\partial r}\right) + \Omega_{ox} \tag{3}$$

with the following initial conditions and boundary conditions:

$$C_{ox}(r, 0) = C_{ox}^{\circ} \tag{4a}$$

$$\frac{\partial C_{ox}}{\partial r}(r_{in}, z) = \frac{\partial C_{ox}}{\partial r}(r_{ou}, z) = 0 \tag{4b}$$

where the possibility of wall reactions has been disregarded.

Assuming that the velocity profile is fully developed we can write

$$v_z(r) = \frac{2Q}{\pi r_{ou}^2(1-\chi^2)}\,\frac{1-(r/r_{ou})^2 + \{(1-\chi)/\ln(1/\chi)\}\ln(r/r_{ou})}{1+\chi^2-(1-\chi^2)/\ln(1/\chi)} \tag{5}$$

where $\chi = (r_{in}/r_{ou})$.

Considering the kinetic characteristics of the reacting system described above, Ω_{ox} may be written as

$$\Omega_{ox} = -H(C_{ox})\Phi e^{a} \tag{6}$$

where Φ is an overall quantum yield and the Heaviside function indicates that the reaction is of zeroth order with respect to the oxalic acid concentration.

The expression for the local volumetric rate of radiant energy absorption (LVREA) is obtained by performing a radiant energy balance where a radiation source model, together with a constitutive equation for the absorption process, must be incorporated.

The emission characteristics of the lamp adopted for the experimental test (non-fluorescent UV arc lamp) required the VEES model [16] to be used. The SELS model [3] could also have been used but the precision required in this work made us feel that the VEES model would provide more reliable answers. Romero *et al.* [17] made a detailed study of these aspects and the reader is referred to their work.

Based on the semiempirical criteria derived for gas–liquid systems [13, 14] and the characteristics of the lamp used, we are able to model the absorption process with equations that are valid for homogeneous media because the value of the napierian absorption coefficient of the pure liquid is higher than 0.4 cm^{-1} [18]. At the same time, in this particular case, the

TABLE 2

Wavelength characteristics of lamp emission and reacting solution napierian absorption coefficients

Wavelength (Å)	*Maximum lamp emission* (einstein s^{-1})	$\mu_{solution}$ [a] (cm^{-1})
2300	—	14.69
2537	7.64×10^{-6}	6.93
3000	2.17×10^{-8}	1.64
3500	1.26×10^{-8}	0.12

[a] $C_{ur} = 10^{-6}$ g mol cm^{-3} and $C_{ox} = 5 \times 10^{-6}$ g mol cm^{-3}.

reacting system can be modelled on the basis of emission data for a single wavelength. In fact, this is a very good approximation only for very specific situations. Table 2 illustrates that here the combination of the radiation source output power and variations in the napierian absorption coefficient with respect to wavelength makes the inclusion of emissions other than those at $\lambda = 2537$ Å meaningless.

The LVREA expression provided by the VEES model, for monochromatic radiation in a homogeneous medium, is [17]

$$e_\nu^{a} = \frac{E_{L,\nu}}{4\pi V_L} \mu_\nu \int_{\phi_1}^{\phi_2} \Delta(\phi) \int_{\theta_1(\phi)}^{\theta_2(\phi)} \exp\left\{ - \int_{\Gamma_{in}(\theta,\phi)}^{\Gamma(\theta,\phi)} \mu_\nu \, d\Gamma \right\} \tag{7}$$

where

$$\Delta(\phi) = 2(r_L^2 - r^2 \sin^2\phi)^{1/2} \tag{8}$$

In developing these equations it has been assumed that each volume element of the lamp emits isotropically an amount of energy proportional to its extent. The resulting e_ν^{a} expression is a function of the spatial variables r and z. A cylindrical coordinate system is used as indicated in Fig. 2. However, the calculation of the radiation energy arriving from all directions in space and from the whole volume of the lamp is performed in a spherical coordinate system located at the point where the LVREA is being evaluated.

In eqn. (7)

$$\Gamma_{in}(\theta, \phi) = \frac{r_{in}}{\sin \theta(\phi)} \tag{9}$$

$$\Gamma(\theta, \phi) = \frac{r}{\sin \theta(\phi)} \tag{10}$$

It should be noticed that the three-dimensional nature of the emission process causes the reactor to be partially irradiated at the incoming and outgoing regions (Fig. 1). Consequently, for each point of incidence inside the reactor volume (designated by $I(r, z)$), we have to determine which

portion of the lamp is irradiating that point. Following the ideas proposed by Romero *et al.* [17], for our case, such a portion of the lamp is adjusted by the integration limits of the θ coordinate (Fig. 2). Figure 3 summarizes the different physical situations with the corresponding integration limits of the θ coordinate.

The θ_i ($i = 1 - 6$) limiting angles are calculated with the following equation:

$$\tan \theta_i = \frac{r \cos \phi + (-1)^{n_i}(r_i^2 - r^2 \sin^2\phi)^{1/2}}{z_i - z} \tag{11}$$

where the values of r_i, z_i and n_i are listed in Table 3.

As shown by eqn. (7), a value of the lamp length is needed by the model. According to the lamp–reactor arrangement for practical annular reactors this length could be equal to or different from the nominal lamp length. In our case and especially because the lamp is located very close to the inner wall of the annular reactor, the general expression for the

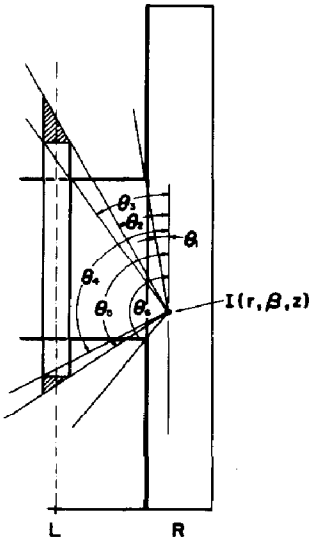

Fig. 2. Limits for the θ coordinate owing to lamp and reactor wedges.

TABLE 3

Values used in eqn. (11)

i	r_i	z_i	n_i
1	r_{in}	z_{L2}	1
2	r_L	z_{L2}	1
3	r_L	z_{L2}	2
4	r_L	z_{L1}	2
5	r_L	z_{L1}	1
6	r_{in}	z_{L1}	1

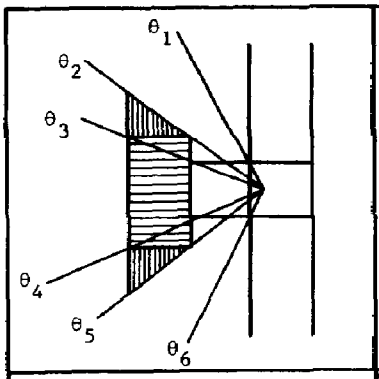

$\theta_1 \leq \theta_2$ and $\theta_6 \geq \theta_5$

Integration limits are:

$[\theta_2 , \theta_5]$

Corrections to account for the effective vertical length of the lamp must be made in the interval:

$[\theta_4 , \theta_5]$ and $[\theta_2 , \theta_3]$

L R	Upper section of the reactor (see figure)	Lower section of the reactor (a symmetric figure)
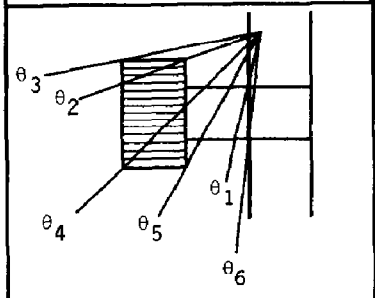	$\theta_1 > \theta_5$	$\theta_6 < \theta_2$
	There are no radiation contributions.	
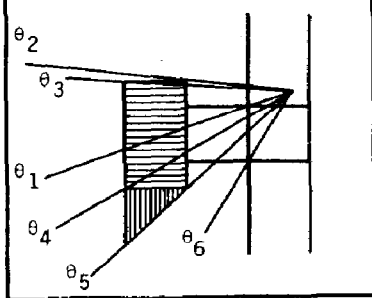	$\theta_3 \leq \theta_1 \leq \theta_4$	$\theta_3 \leq \theta_6 \leq \theta_4$
	Integration limits are:	
	$[\theta_1 , \theta_5]$	$[\theta_2 , \theta_6]$
	Corrections must be also made but only in the regions limited by:	
	$[\theta_4 , \theta_5]$	$[\theta_2 , \theta_3]$
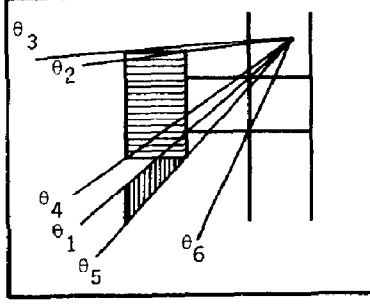	$\theta_4 \leq \theta_1 \leq \theta_5$	$\theta_2 \leq \theta_6 \leq \theta_3$
	Integration limits are:	
	$[\theta_1 , \theta_5]$	$[\theta_2 , \theta_6]$
	Corrections must be also made along the whole interval.	

Fig. 3. Limits for the θ coordinate; description of characteristic cases.

limiting angles of θ as derived by Irazoqui *et al.* [1] must be modified. In fact if no corrections were introduced we would compute as emission volumes portions of a cylinder which correspond to regions in the space

where there is no emission at all (shaded portions in Fig. 2 and Fig. 3). This effect is significant (as it is also in the case of the wedges at both reactor ends) when the inner reactor wall is close to the lamp. A function η is defined which accounts for the lamp wedges:

$$\eta(\theta, \phi) = \frac{(z_j - z) \tan \theta - r \cos \phi + (r_L{}^2 - \sin^2\phi)^{1/2}}{2(r_L{}^2 - \sin^2\phi)^{1/2}} \tag{12}$$

where $z_j = z_{L2}$ for the upper lamp wedge and $z_j = z_{L1}$ for the lower lamp wedge.

Hence, using the η function, the LVREA expression becomes

$$e_\nu{}^a = \frac{E_{L,\nu}\mu_\nu}{4\pi V_L} \int_{\phi_1}^{\phi_2} \Delta(\phi) \int_{\theta_1}^{\theta_2} \eta(\theta, \phi) \exp\left\{ - \int_{\Gamma_{in}(\theta,\phi)}^{\Gamma(\theta,\phi)} \mu_\nu \, d\Gamma \right\} \tag{13}$$

Figure 3 also shows the cases where the correction is required. In the remaining cases, η must be equal to one.

Finally, the limits for ϕ are [17]

$$-\phi_1 = \phi_2 = \cos^{-1}\left\{1 - \left(\frac{r_L}{r}\right)^2\right\} \tag{14}$$

Equations (8) - (14) are used to calculate the monochromatic local volumetric rate of energy absorption. The final value of Φe^a required by eqn. (6) is obtained by performing an integral over the whole range of emitting frequencies of the lamp:

$$\Phi e^a = \int_\nu \Phi_\nu e_\nu{}^a \, d\nu \tag{15}$$

Since the napierian absorption coefficient of the absorbing species is assumed to remain constant during the reaction [11], the LVREA can be evaluated independently of the information provided by the mass balance equation.

In spite of this simplification in the mathematical treatment, the remaining equations, eqns. (3) - (6), cannot be solved analytically. The numerical procedure followed in the solution, particularly to compute the three-dimensional attenuation process, has been described in detail by Romero *et al.* [17] and will not be repeated here.

Once the oxalic acid concentration field inside the reactor is known, we can calculate the average exit conversion to compare it with the experimental results. The average exit conversion is computed as follows:

$$\langle x_{ox} \rangle = 1 - \frac{\langle C_{ox} \rangle}{C_{ox}{}^o} \tag{16}$$

and

$$\langle C_{ox} \rangle = \frac{1}{Q} \int_{r_{in}}^{r_{ou}} 2\pi r v_z(r) C_{ox}(r, L) \, dr \tag{17}$$

5. Results and discussion

Figures 4(a) and 4(b) show, for reactors 1 and 2 respectively, a comparison between the experimental results and the theoretical predictions estimated using the VEES model. The full line indicates the theoretical values obtained using the maximum UV output power (after operation for 100 h, Table 1). The broken line corresponds to the calculations using the average UV output power "through life" (Table 1). Both values are nominal specifications provided by the lamp manufacturer [15].

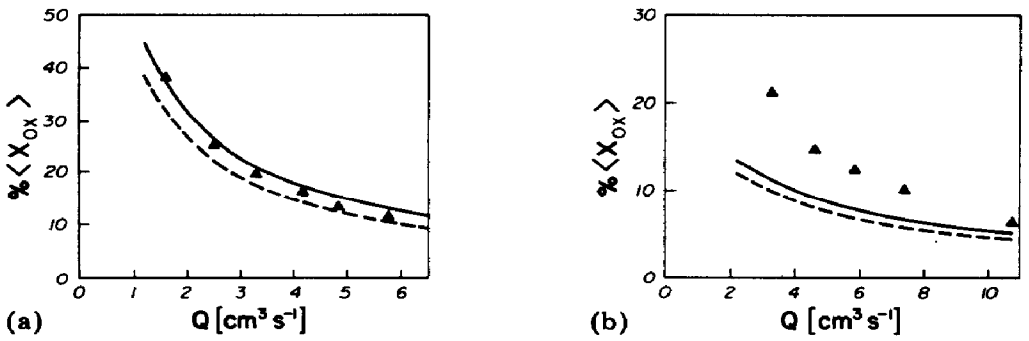

Fig. 4. Theoretical predictions and experimental results with constant napierian absorption coefficient: (a), reactor 1; (b), reactor 2.

It should be expected that experimental values will fall below the full line (Figs. 4(a) and 4(b)), at least for conversion values lower than 20% which is the maximum figure recommended for the actinometric reaction [11, 12]. It is interesting to note that two recommendations have been made quite a long time ago regarding the experimental operating conditions, *i.e.* (1) the maximum permissible value of conversion and (2) the requirement of very good stirring. We can interpret (1) as indicating the possibility of changes in the validity of the reaction rate expression when the conversion is greater than 20% and (2) as indicating the necessity of fulfilling the conversion restriction not only for the averaged exit conversion but also for all the local values inside the reactor.

The experimental behavior can be seen in Figs. 4(a) and 4(b). The former, for reactor 1, seems to reproduce at least approximately the expected results. It is clear that the predictions are no longer valid for reactor 2.

In a continuous laminar flow reactor without mixing, concentration gradients are unavoidable, mainly in the radial direction where the LVREA variations are more noticeable. Hence, although the average exit conversion was kept below 20%, it is possible that in certain regions inside the reacting volume the local conversion exceeded this value.

Figure 5 shows the radial LVREA profiles for reactors 1 (full line) and 2 (broken line). Steep radial gradients in the radiation field are observed, especially in reactor 2 where the LVREA profile shows a variation of four orders of magnitude in the space between the inner and outer radii (with

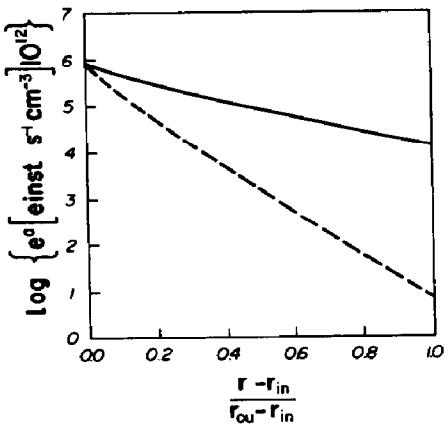

Fig. 5. Radial profiles of the local volumetric rate of energy absorption for reactor 1 (———) and reactor 2 (— — —).

$r_{ou} - r_{in} = 13$ mm). Thus, high conversion gradients should be expected in the same direction. In Figs. 6(a) and 6(b) radial conversion profiles at the halflength of reactors 1 and 2 respectively are plotted for different values of the volumetric flow rate. Both figures show that the local values of the oxalic acid conversion are always higher than 20% in the regions close to the entrance of light.

When most of the oxalic acid has been consumed, we may have at least three effects that have not been accounted for.

(I) During the reaction, while the oxalic acid concentration decreases, a change in the chemical nature of the absorbing species should be expected, particularly when the acid concentration falls to zero. It is also known that the addition of oxalic acid to uranyl ions increases the absorption properties of the resulting solution [10]. Therefore, the napierian absorption coefficient may be a function of composition. It seems plausible that the main reason for the disagreement between experimental and theoretical results shown in Figs. 4(a) and 4(b) could be the invalidation of the hypothesis

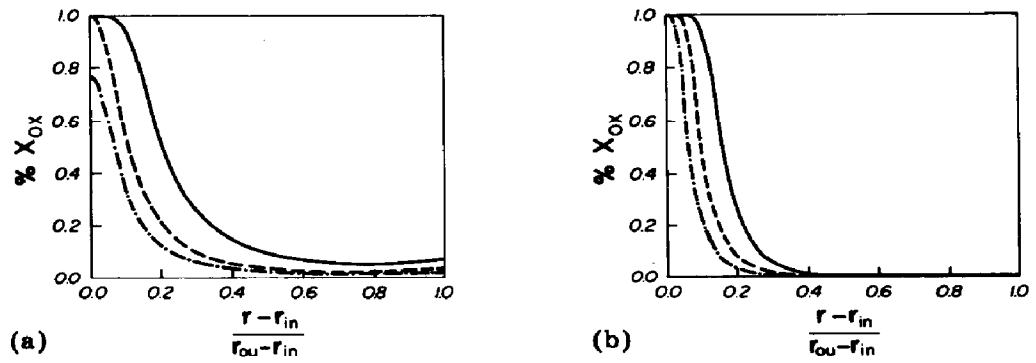

Fig. 6. Radial profiles of the oxalic acid conversion calculated with constant napierian absorption coefficient at $z = (z_{R1} + z_{R2})/2$. (a) Reactor 1: $Q = 1.67$ cm^3 s^{-1} (———); $Q = 4.17$ cm^3 s^{-1} (— — —); $Q = 6.67$ cm^3 s^{-1} (— · —). (b) Reactor 2: $Q = 2.50$ cm^3 s^{-1} (———); $Q = 6.67$ cm^3 s^{-1} (— — —); $Q = 15.00$ cm^3 s^{-1} (— · —).

of a constant napierian absorption coefficient when conversion values are higher than 20%. Since the attenuation process occurs from the inner wall (the surface at which the radiation enters) to the point of incidence, the theoretical calculations of the LVREA for the whole reactor volume could also be invalidated.

It is clear that it is almost impossible to avoid operating the reactor with very high conversions in regions close to the inner wall (the exception would be the impractical case of using a very low optical thickness). However, it seems that predictions can still be fairly good if the characteristic radiation path length is short because the concentration gradients are smoother and the regions of the reactor subject to incorrect predictions are considerably less significant when compared with the total reactor volume. This applies to reactor 1. When the characteristic radiation path length is longer (reactor 2), the concentration gradients are so steep that almost all regions of the reactor are operating under conditions where the reaction rate is predicted incorrectly. Figure 6(b) shows that in fact a large proportion of the reactor volume receives such low values of energy that the reactant circulates through it with negligible reaction effects.

(II) When most of the oxalic acid has been consumed, the uranyl ion could undergo secondary reactions: mainly changes in its oxidation state [10]. Thus a change in the reaction mechanism could be expected that would certainly affect the information used in the predictions of the reactor model.

(III) When conversions are greater than 75% - 80%, it is known that the values of the quantum yield could be affected [11]. Consequently, the local values of Φ used in the model would no longer be correct.

5.1. Variable napierian absorption coefficient

Since the uranyl ion concentration remains constant during a large part of the reaction, variations in the napierian absorption coefficient should result from changes in the oxalic acid concentration. A simple experimental test was devised to verify this hypothesis. The absorbance of solutions of various concentrations of oxalic acid but a constant concentration of uranyl ion were spectrophotometrically measured at different wavelengths. Figure 7 shows the results.

It should be noticed that the napierian absorption coefficient remains almost constant when the oxalic acid concentration is greater than 0.004 M. Hence, the plot shows the expected behavior, *i.e.* starting with a solution of composition 0.001 M uranyl sulfate and 0.005 M oxalic acid the hypothesis of a constant napierian absorption coefficient is satisfied only if the reaction proceeds without reaching conversions greater than 20%. The oxalic acid concentration effect is very noticeable at short wavelengths. In fact, for values of $\lambda > 3000$ Å these restrictions are less severe (Fig. 7). In our case the combination of the characteristics of the lamp emission and the absorption properties of the reacting solution rendered the hypothesis unacceptable (Table 2).

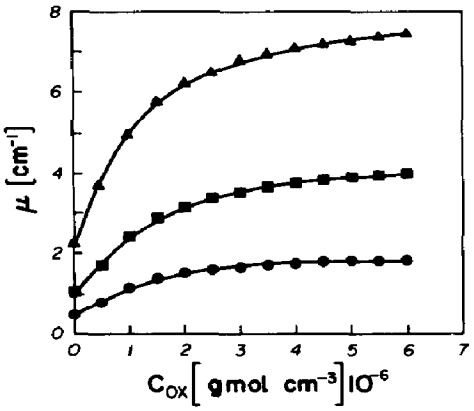

Fig. 7. Napierian absorption coefficient as a function of the oxalic acid concentration with $C_{ur} = 10^{-6}$ g mol cm^{-3}: (▲), 2537 Å; (■), 2800 Å; (●), 3000 Å.

The theoretical predictions were repeated using the new absorption data. Since the napierian absorption coefficient is now a function of the oxalic acid concentration, there is a coupling between the mass balance equation and the evaluation of the radiant energy field which considerably increases the complexity of the computational problem, as shown by Romero *et al.* [17].

The radial conversion profiles plotted in Figs. 6(a) and 6(b) were recalculated using a variable napierian absorption coefficient and Figs. 8(a) and 8(b) depict the results: Fig. 8(a) shows that under the new conditions conversions do not reach such high local values, not even at places close to the inner reactor wall. But from Fig. 7 we also know that when the conversion increases, the napierian absorption coefficient decreases. This produces a better penetration of the energy inside the reactor and a more uniform concentration field in the radial direction. However, Fig. 8(b) does not show much improvement as far as the radial concentration profiles are concerned. The requirement that conversions higher than 5% be achieved (to minimize errors in the chemical analysis of the reaction products) imposes, in some cases, high mean residence times. In fact, the situation is really improved only for large flow rates. When the mean residence time is long, total conversion in regions closer to the entrance of radiation is unavoidable. Under these conditions the uranyl oxalate complex ion does not exist any longer and the napierian absorption coefficient is that corresponding to the uranyl ion alone. Moreover, if this is the case, departures from the initial assumptions as indicated by (II) and (III) above will become significant. Thus, for very high values of the mean residence time, the predictions of the model should show considerable differences from the experimental values, while they should show good agreement as the mean residence time is shortened. Unfortunately, the literature does not provide quantitative information about the behavior of the reaction when conversions are higher than 80%. Consequently, the *a priori* predictions for these extreme conditions cannot be improved.

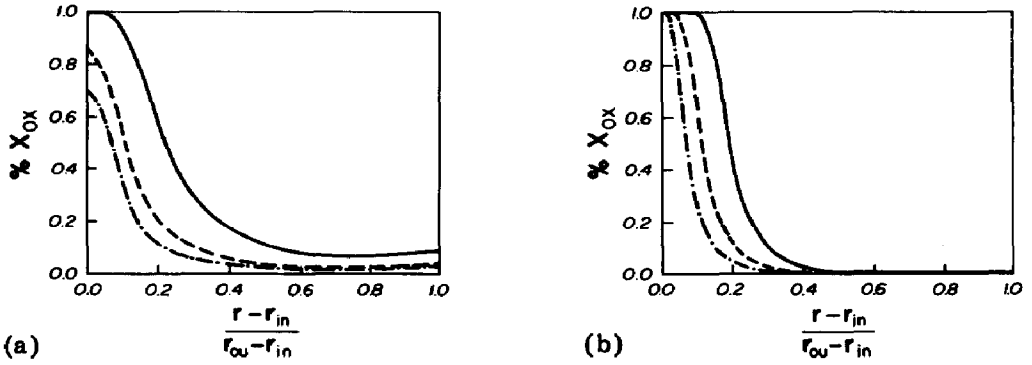

Fig. 8. Radial profiles of the oxalic acid conversion estimated with variable napierian absorption coefficient at $z = (z_{R1} + z_{R2})/2$. (a) Reactor 1: $Q = 1.67$ cm^3 s^{-1} (———); $Q = 4.17$ cm^3 s^{-1} (— — —); $Q = 6.67$ cm^3 s^{-1} (— · —). (b) Reactor 2: $Q = 2.50$ cm^3 s^{-1} (———); $Q = 6.67$ cm^3 s^{-1} (— — —); $Q = 15.00$ cm^3 s^{-1} (— · —).

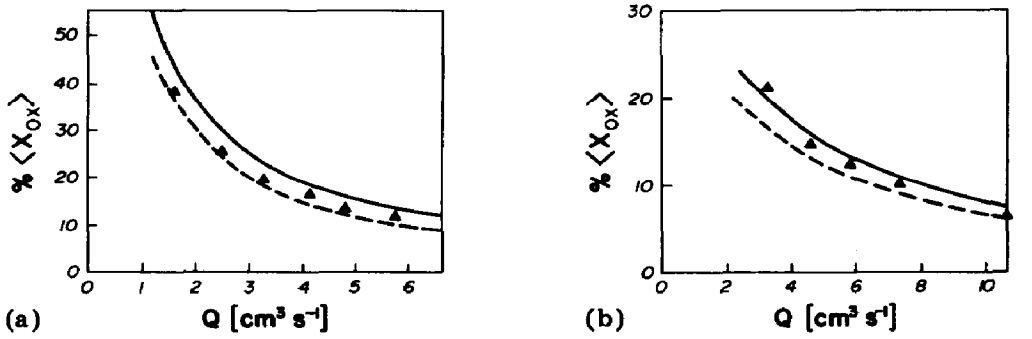

Fig. 9. Theoretical predictions and experimental results with a variable napierian absorption coefficient: (a) reactor 1; (b) reactor 2; ———, theoretical predictions using maximum output power; — — —, predictions using average UV output power through life.

Figures 9(a) and 9(b) show results calculated with a variable napierian absorption coefficient and provide surprisingly good corroboration of the expected results in the light of the above discussion. Again, the full line represents the theoretical predictions obtained using the maximum UV output power (after operation for 100 h, Table 1), while the broken line corresponds to the predictions using the average UV output power through life (Table 1). The point that lies above the full line corresponds to a reactor operating condition where oxalic acid conversions close to unity are produced in significant portions of the reactor volume.

6. Conclusions

(1) Using the VEES model together with the lamp specifications provided by the manufacturer, the geometrical characteristics of the reactor–lamp device and the optical and kinetic properties of the reacting solution, we were able to make very precise predictions of the exit conversion of a

kinetically simple photochemical reaction in a continuous annular photochemical reactor.

These results, together with those reported previously [4 - 6] for different geometries, undoubtedly show the ability of the VEES model to predict the radiant energy distribution inside a reactor. This allows us to produce an *a priori* design of a photochemical reactor, at least for simple reactions.

(2) Special care should be taken when, in order to analyze the radiation field inside a segregated flow continuous reactor, a uranyl oxalate actinometer is used. It is impossible to avoid operating at very high conversions in certain regions of the reacting volume. If accurate predictions are required and the evaluation of the LVREA is performed under the hypothesis of a constant napierian absorption coefficient, the oxalic acid conversion must be kept below the maximum permissible value of 20% at any point inside the reactor volume. This is critical if the lamp emission is very strong at short wavelengths where the effect of the oxalic acid concentration is very important. However if in the theoretical calculation the napierian absorption coefficient is allowed to be a function of the oxalic acid concentration, the local conversion values may be as high as 75% - 80%.

(3) When the reaction is used to measure the radiation field, *i.e.* no model is used to compute the radiation, very good stirring is required to avoid high local values of conversion that invalidate the known values of μ and Φ. If conversions are greater than 20% and significant lamp power outputs are produced at short wavelengths ($\lambda < 3000$ Å) a variable napierian absorption coefficient must be used. Then, no advantage exists in using this reaction since the potassium ferrioxalate actinometer has the same requirement ($\mu = \mu(c)$) and it is much more sensitive by far [19 - 22].

Acknowledgments

The authors wish to thank Mr. José Luis Giménez for his valuable participation in the experimental work. They are also grateful to Professor Elsa I. Grimaldi for her revision of the English version of the work. Finally, we acknowledge the financial aid received from the National Council for Scientific and Technological Research of Argentina and from Universidad Nacional del Litoral (Santa Fe, Argentina).

Nomenclature

C concentration (g mol cm^{-3})
D diffusion coefficient ($cm^2\ s^{-1}$)
e^a local volumetric rate of energy absorption (einstein $s^{-1}\ cm^{-3}$)
E radiant energy flow rate (einstein s^{-1})
L length (cm)

Q volumetric flow rate ($cm^3\ s^{-1}$)
r cylindrical coordinate (cm)
v velocity ($cm\ s^{-1}$)
V volume (cm^3)
x conversion
z cylindrical coordinate (cm)

Greek symbols
Γ linear coordinate along the radiation path (cm)
Δ defined by eqn. (8)
η defined by eqn. (12)
θ spherical coordinate
χ ratio of the inner to the outer radius (dimensionless)
μ napierian absorption coefficient ($cm^2\ g\ mol^{-1}$)
ϕ spherical coordinate
Φ overall quantum yield ($g\ mol\ einstein^{-1}$)
Ω reaction rate ($g\ mol\ s^{-1}\ cm^{-3}$)

Subscripts
in inner reactor wall
L radiation source
ox oxalic acid
ou outer reactor wall
R reactor
ur uranyl ion
z axial coordinate
ν monochromatic property

Superscripts
° inlet section

Special symbols
$\langle\rangle$ average value

References

1 H. A. Irazoqui, J. Cerdá and A. E. Cassano, *AIChE J., 19* (1973) 460.
2 C. Stramigioli, F. Santarelli and F. P. Foraboschi, *Ing. Chim. Ital., 11* (1975) 143.
3 S. M. Jacob and J. S. Dranoff, *Chem. Eng. Prog., Symp. Ser., 62* (1966) 47.
4 J. Cerdá, J. L. Marchetti and A. E. Cassano, *Lat. Am. J. Heat Mass Transfer, 1* (1977) 33.
5 E. R. De Bernardez and A. E. Cassano, *Lat. Am. J. Heat Mass Transfer, 6* (1982) 333.
6 O. M. Alfano, R. L. Romero and A. E. Cassano, in L. K. Doraiswamy and R. A. Mashelkar (eds.), *Frontiers in Chemical Reaction Engineering*, Vol. 1, Wiley, New Delhi, 1984, p. 506.
7 W. G. Leighton and G. S. Forbes, *J. Am. Chem. Soc., 52* (1930) 3139.
8 G. S. Forbes and L. J. Heidt, *J. Am. Chem. Soc., 56* (1933) 2363.

9 D. H. Volman and J. R. Seed, *J. Am. Chem. Soc., 86* (1964) 5095.
10 L. J. Heidt, G. M. Tregay and F. A. Middleton, *J. Phys. Chem., 74* (1970) 1876.
11 W. A. Noyes and P. A. Leighton, *The Photochemistry of Gases*, Reinhold, New York, 1941, p. 82.
12 P. Borrel, *Photochemistry. A primer. Studies in Chemistry 8*, Arnold, London, 1973, p. 29.
13 T. Otake, S. Tone, K. Higuchi and K. Nakao, *Kagaku Kogaku, 7* (1981) 57.
14 T. Yokota, T. Iwano, H. Deguchi and T. Tadaki, *Kagaku Kogaku, 7* (1981) 157.
15 *Tech. Bull. TP-122*, 1967, (General Electric Company).
16 O. M. Alfano, R. L. Romero and A. E. Cassano, in Mujumdar and R. A. Mashelkar (eds.), *Advances in Transport Processes*, Vol. 4, Wiley Eastern, New Delhi, 1985, p. 201.
17 R. L. Romero, O. M. Alfano, J. L. Marchetti and A. E. Cassano, *Chem. Eng. Sci., 38* (1983) 1593.
18 A. E. Cassano, *Rev. Fac. Ing. Quim., 37* (1968) 469.
19 C. A. Parker, *Proc. R. Soc. London, Ser. A, 220* (1953) 104.
20 J. H. Baxendale and N. K. J. Bridge, *J. Phys. Chem., 59* (1955) 783.
21 C. G. Hatchard and C. A. Parker, *Proc. R. Soc. London, Ser. A, 235* (1956) 518.
22 J. G. Calvert and J. N. Pitts, Jr., *Photochemistry*, Wiley, New York, 1966.